An Ambient Detection System for Visualization of Charged Particles generated with Ionization Methods at Atmospheric Pressure

Bob Hommersom[a,b], Sarfaraz U.A.H. Syed[a,d], Gert B. Eijkel[a,b], David P.A. Kilgour[c], David R. Goodlett[c,e], Ron M.A. Heeren[a,b,d]

[a]FOM Institute AMOLF, Science Park 104, 1098 XG Amsterdam, The Netherlands

[b] M4I, The Maastricht MultiModal Molecular Imaging Institute, University of Maastricht, Universiteitssingel 50, 6229 ER Maastricht, The Netherlands

[c]University of Maryland School of Pharmacy, Baltimore, Maryland, USA

[d]Amsterdam Scientific Instruments B.V., Science Park 105, 1098 XG Amsterdam, The Netherlands

[e]Deurion LLC, Seatle, WA, USA

Address reprint requests to:
Prof. Dr. Ron. M. A. Heeren
M4I, Maastricht University
Universiteitssingel 50
6229 ER Maastricht
The Netherlands

Rationale

With the current state of the art detection of ions only taking place under vacuum conditions active pixel detectors that operate under ambient conditions are of particular interest. These detectors are ideally suited to study and characterize the charge distributions generated by ambient ionization sources.

Methods

The direct imaging capabilities of the active pixel detector are used to investigate the spatial distributions of charged droplets generated by three ionization sources, named electrospray ionization (ESI), paper spray ionization (PSI) and surface acoustic wave nebulization (SAWN). The ionization spray (ESI/PSI) and ionization plume (SAWN) originating from each source is directly imaged. The effect of source parameters such as spray voltage for ESI and PSI, and the angle of the paper spray tip on the charge distributions is investigated. Two types of SAWN liquid interface, progressive wave (PW) and standing wave (SW) are studied.

Results

Direct charge detection under ambient conditions is demonstrated using an active pixel detector. Direct charge distributions are obtained of weak, homogeneous/focussed and dispersed spray plumes by applying low, intermediate and high spray potentials, respectively, for ESI. Spray plume footprints obtained for various angles of PSI shows the possibility to focus the ion beam as a function of the paper angle. Differences between two designs of the SAWN interface are determined. Droplet charge flux changes are illustrated in a way similar to a total ion chromatogram.

Conclusions

The use of this active pixel detector allows the rapid characterization and optimization of different ambient ionization sources without the actual use of a mass spectrometer. Valuable illustrations are obtained of changes in spatial distribution and number of charges detected for ESI, PSI and SAWN ion plumes.

1. Introduction

Mass spectrometry (MS) has become one of the most sensitive, accurate and informative analytical tools for a broad community. The use of mass spectrometry (MS) has flourished in both industry and research, with applications ranging from analysis of simple residual gas mixtures to complex organic materials, providing an imposing testimony to the value of this technique.[1,2] The desire to mass spectrometrically analyze large numbers of samples at the point-of-use in the areas of biomedical, clinical, environmental research and public safety monitoring led to the development of ambient ionization techniques. The capabilities of ambient ionization (AI) methods are particularly well suited to these high volume applications in that sample preparation is minimized and/or not required.[3] Ambient Ionization mass spectrometer (AI-MS) methods have shown extraordinary performance due to their simplified analysis procedures.

AI-MS is considered to be a relatively new paradigm that facilitates both sampling and ionization of analyte(s) under ambient conditions with little or no sample preparation.[4] However, electrospray ionization,[5] first presented in 1984, could be argued to be the first AI-MS technique, since it generates ions at atmospheric pressure. Since this time, many other ambient ionization techniques have emerged. Techniques such as desorption electrospray ionization (DESI),[6] direct analysis in real time (DART), plasma-assisted desorption/ionization (PADI) and low temperature plasma (LTP) probes have all demonstrated their usefulness. More recently, simplified, low-cost AI techniques such as surface acoustic wave ionization (SAWN) and paper spray ionization (PSI) have also been developed.

In SAWN, a surface acoustic wave is used to transfer energy into a liquid droplet resulting in nebulization of the liquid.[7] This nebulized plume can be aspirated into a mass spectrometer where various mechanisms can result in the production of ions.[8–11] The mechanism of SAWN ionization is considered to be similar to the statistical charge imbalance methods[12,13] which produce ions from other unbiased droplet ionization sources, such as thermospray,[14,15] sonic spray,[16] from droplets produces by focused sonic waves or the bursting of bubbles at the surface of a liquid.[17]

PSI, developed in 2010, uses filter paper cut in a triangle shape and wetted with a small volume (< 10 µL) of solution.[18] Analyte(s) can be preloaded onto the paper and ions are generated by applying a high voltage to a paper triangle. The mechanism for the extraction of droplets from the edge of the paper and the subsequent production of ions from the droplets is thought to be similar to the mechanisms seen in nanoelectrospray.[19,20]

Almost all current state of the art ion detection systems used in mass spectrometry operate under high or ultra-high vacuum. In order to characterize and optimize ambient ionization sources for mass spectrometry, investigations into the optimum source operating conditions are typically carried out by measuring the signal at the end of the mass spectrometer. In some cases, the ionization plume evolving from AI sources has been studied experimentally under ambient conditions using a microscopic camera,[21] or water sensitive paper.[22] Theoretical investigations of AI sources using simulation tools such as COMSOL[23] have been reported in the past. However, none of the empirical methods used in the study of AI sources under ambient conditions gives an accurate intensity profile along with visualization (i.e. spatial information) of the charge distribution in the evolving ionization plume.

Previously, the use of a new imaging detector (Timepix) has been demonstrated with MS technologies such as quadrupole mass spectrometry[24] and Secondary Ion Mass Spectrometry (SIMS)[25] on a time of flight instrument. We hypothesized that as the Timepix detector can operate at ambient pressure it could be used to detect and image the liquid plumes generated by a variety of atmospheric pressure liquid interfaces for mass spectrometry such as electrospray, paper-spray and SAWN. If the spray plume could be imaged then Timepix offers the opportunity to study or quantify the processes or characteristics of the plume and would also provide feedback that could be used to optimize the interface conditions.

2. Methods

Techniques of ionization

Electrospray Ionization

Electrospray produces ions by applying an electric field to a solution passing, with a weak flux, through a capillary tube from which the solution is nebulized to form a spray of small charged droplets at, or near, atmospheric pressure. Two models exist to explain the ion generation process, known as ion evaporation model (IEM)[26] and charge residue model (CRM).[27] In the IEM the electric field strength at the surface of the droplet reaches a certain point at which solvated ions are expelled. In the CRM the droplets experience evaporation and fission cycles; as the droplets become smaller due to solvent evaporation, increasing ion-ion repulsion leads to droplet fission. This reduction in droplet size followed by fission continues until individual ions, pre-formed in the solution, appear in the gas phase. The current thought is that both models are true – but that IEM dominates for small ions and CRM for large ions. For experiments with electrospray, the needle is placed horizontally in front of the Timepix detector. The tip diameter (ID) of the ESI needle is 20 µm. The flow rate is 36 µL/hr. Electrolyte solutions with a standard ratio of 1:1 H_2O and MeOH were used. No sheath gas has been used. The distance between source and detector is fixed at 0.5 cm. The spray plume is generated and will be detected upon arrival at the Timepix detector.

Paper Spray Ionization

Paper spray ionization makes use of paper, macroscopically cut to a sharp point, as a fluid reservoir and transportation material.[18] Samples can be preloaded or pre-absorbed by the paper before wetting it with a solvent to make it conductive.[19] The sharp point establishes a high electric field at the tip needed to cause the liquid to form an electrospray resulting in ionization.[23] Whatman paper (Whatman cellulose filters, Sigma Aldrich, Grade 1, USA) with a thickness of 180 µm is used. High voltage is applied by means of a clamp at the bottom of the paper triangle, thereby positioning the paper horizontally and directly pointing it at the Timepix detector. The distance between paper and detector is fixed at 0.5 cm. In the experiments reported here with paper spray, we have used paper triangles with a base of 1 cm and a tapered cone with four different angles of 30°, 45°, 60° and 90° respectively. The paper is pre-wetted with a volume < 10 µL of an electrolyte solution with a standard ratio of 1:1 H_2O and MeOH.

SAWN

The SAWN chips used here had interdigitated transducers (IDT) printed in gold on top of a lithium niobate piezoelectric wafer by a previously described photolithographic process.[8] An alternating potential of 10MHz is applied to the IDTs via a signal amplifier. Two versions of the SAWN chip are available; one that generates a progressive wave (PW) in the surface of the piezoelectric wafer. The second generation of chips has two IDTs printed facing each other. In the latter case two traveling waves are generated, thereby creating a standing wave (SW) between the transducer arrays. For PW chips a sample aliquot is deposited on the surface of the SAWN chip in the path of the IDT produced SAW or in the case of the SW chips in the center spot between the IDTs. When subjected to the SAW, the liquid is desorbed and charged, resulting in a droplet/ion cloud having a kinetic energy component directed upwards, toward the Timepix detector. The detector is positioned 1 cm above the SAWN chip. This ionization method has proven to work with mass spectrometric analysis when the SAWN chip was positioned below the atmospheric pressure inlet of the mass spectrometer.[9] For this experiment, an additional electrode was printed on the chip, in the path of the wave, to allow an external potential to be applied to the liquid aliquot deposited on the SAWN chip prior to nebulization in order to increase the number of excess charges on the surface of the droplets produced as a result of nebulization. Electrolyte solutions with a standard ratio of 1:1 H_2O and MeOH were used with 0%, 1% and 10% NH_4OH.

Charge distribution determination

The Medipix2[28]/Timepix chips[29] are active pixel detectors developed by the Medipix collaboration and hosted by CERN (Medipix collaboration, www.cern.ch/medipix). The Medipix/Timepix family has found its way into MS, e.g. for imaging and diagnostic purposes of TOFMS instruments.[30,31] The in vacuum use of these detector involves the placement of microchannel plates (MCPs) in front of the Timepix read-out chip.[32] The impact of ions exiting the mass analyser on the MCPs produces electron showers which are subsequently detected by the readout chip. The dimension of an individual Medipix/Timepix chip is 1.4×1.6 cm^2. The major characteristics of this application-specific integrated circuit (ASIC) are 256×256 pixels, with a pitch of 55 µm, no electronic noise and pixel level functionality. Here, we have used the Timepix chip without preceding MCPs. This enables direct charge detection under atmospheric conditions.

In this investigation the results are produced using the Timepix chip operating in event counting mode and in Time over Threshold (ToT) mode. In the event counting mode, each pixel registers a count when the number of impinging charges exceeds a pre-set threshold, typically 600 charges. After the charge level drops below the threshold on a pixel the pixel is ready to receive a subsequent event.

In the ToT mode the pixel registers how many clock cycles the pixel remains above a pre-set threshold. As the rate at which the surface of the chip discharges is constant, the time that the chip remains above the threshold is a measure of the amount of charge that was supplied in an event. In addition the spatial information of ions in 2-dimensions (i.e. their x-y positions) is registered.

Whichever mode is used, this generation of the Timepix system can record and store an image of the events which have been recorded by every pixel, at a rate of 10Hz. These images can be thought of as frames in a movie and offer the capability to record how a charged particle stream has varied over time. All images were acquired with a 10 Hz frame rate and a frame acquisition time of 50 ms.

The chip is controlled via a dedicated acquisition and control software and graphical user interface, "Pixelman".[33]

Setup

For both ESI and PSI the spray source is mounted horizontally and the detector vertically, so the spray plume has a direction orthogonal to the plane of detection (see Fig 1a and 1b). An experiment is performed by recording 100 frames under the same conditions.

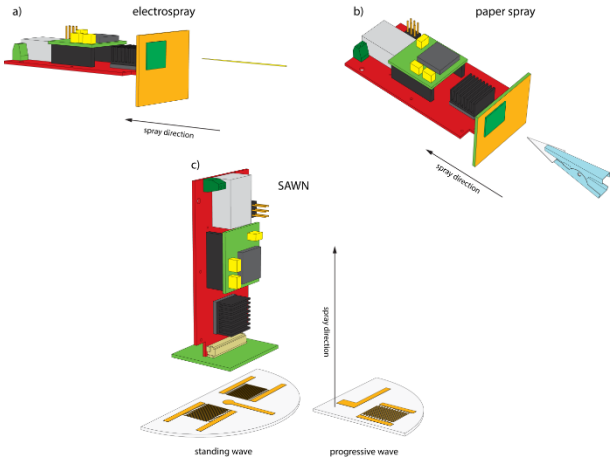

Figure 1 - Illustration of the setups for a) electrospray ionization, b) paper spray ionization, and c) two designs of surface acoustic wave nebulization, progressive wave and standing wave chip design.

For the SAWN experiments the active pixel detector is positioned above the SAWN chip, parallel to SAWN chip so the upward directed plume generated by the SAW is orthogonal to the plane of detection (see Fig 1c for the PW and the SW chip). Various electrolyte solutions were used for the experiments reported with SAWN. For a typical experiment, acquisition of the frames on the detector is started and an aliquot is added on the center spot of the SAWN chip. The nebulized plume is generated and the ion cloud is detected by the Timepix detector. Part of the kinetic energy the charged droplets obtain is predominantly directed upwards with respect to the plane of the SAWN chip. This enables us to analyze the plume with the detector positioned a distance *d* above the SAWN chip. The plume generated by SAWN is however potentially also affected by convection and turbulence. Small flows of air will have impact on the number of detected particles. The setup is shielded to prevent the influence of air flow around the system.

3. RESULTS AND DISCUSSION

Visualization of electrospray ionization

The spray plumes originating from the electrospray needle were analyzed using the Timepix detector at different spray voltages. The generated spray plume travels 0.5 cm towards the detector and is integrated over 100 frames, of 0.1 s/frame and the summed image yields the distribution of the total ion current and the spray footprint. Fig 2 is a 3D representation of a z-stack of 2D contour maps that shows the variation in spatial distribution of the spray plumes for different ESI voltages. We observe a radially dispersed spray plume with higher intensity in the center of the plume at a lower spray

voltage of 2.0 kV. For lower voltages we observe a weak spray that is unstable. An increase in applied spray potential to 3.5 kV leads to better focusing of the spray plume directed at the detector. The focused spray plume shows a more homogeneous distribution in intensity. With a further increase in spray potential to 3.9 kV the ESI plume becomes unstable and separates into multiple sprays that are observed as distinctive lobes in the Timepix image. The effects of space charge will increase with applied potential for the same spray volume. The Coulombic repulsions within the ion plume and the increase in electric field strength determine the extent of the observed effect. Local surface oscillation potentially creates optimal spray conditions at multiple locations. Figure 2 gives a superb illustration of the change in spatial distribution of emitted charges and overall intensity for increasing ESI voltage. The dispersion of the plume at higher ESI voltages results in the decrease of the measured ion intensity detected in the mass spectrometer. The optimal distribution for mass spectrometric analysis is a homogeneously distributed, focused spray, so that with use of the atmospheric pressure inlet a larger population of droplets can directed into the mass spectrometer. This is the case for intermediate spray potentials.

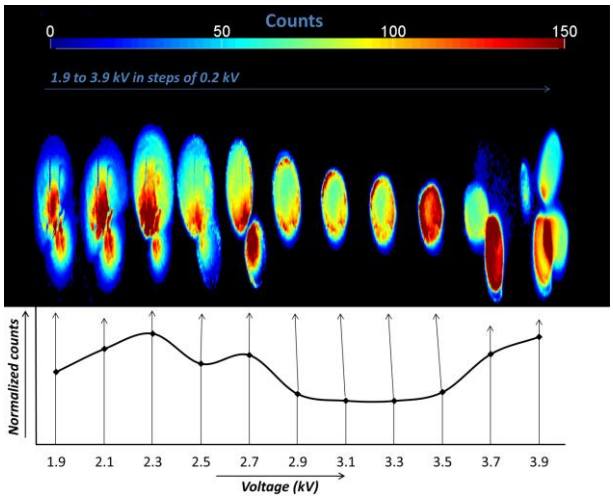

Figure 2 - 3D representation of a z-stack of 2D contour maps showing the development of the ESI ion beam with the spray voltage increasing from 1.9 to 3.9 kV. Counts are represented on a normalized scale with the maximum at 2.3 kV for 294200 counts.

Visualization of paper spray ionization

The spatial distribution and the spray intensity profile of the ionization plume originating from PSI were studied for four different angles of the paper tip. The angle of the paper tips plays a major role in the generation of the spray. Fig. 3 a-d shows the spray plumes for tip angles 30°, 45°, 60°, 90°, respectively. The spray voltage was maintained at 4.6 kV. Each image consists of an integral over 100 acquisition frames measured from the Timepix detector. For the case with 30° paper tip (Fig 3a), multiple spray cones originating from the paper can be observed. The spray plume has an irregular shape with an inhomogeneous intensity distribution. An increase in paper tip angle (45°, Fig. 3b), makes the spray more stable, but multiple cone jets are still visible. It is common to see multiple cone jets with paper spray ionization and the number of multiple jets tend to vary with solvent composition, solvent flow rate and applied spray potential[21] which in turns determines the electric field strength around the paper tip. With a further increase in paper tip angle to 60° (Fig. 3c) and 90° (Fig. 3d), the

spray plume gets more focused. The spray plume has a radial distribution similar to an ESI plume, with an increased intensity on the outside. This can be explained by a high electric field in the center which causes ions of similar polarity to repel each other. The best focusing characteristics were obtained for the case of a tip angle of 90°. Our results, that show better spray plume focusing characteristics and decrease in plume diameter with increasing tip angle, agree with the observations published by Yang et al.[23]

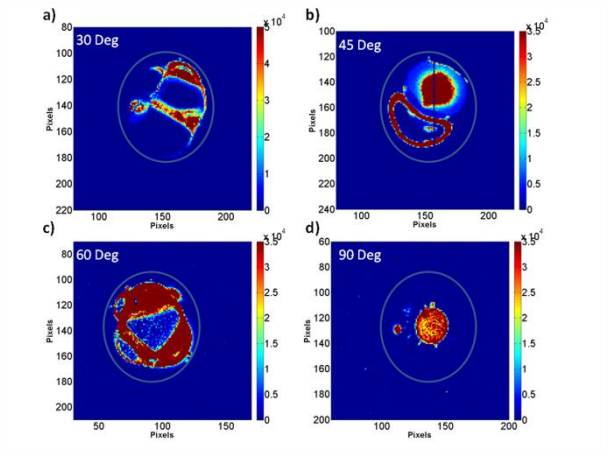

Figure 3 - Paper spray ionization plumes observed for a) 30°, b) 45°, c) 60°, and d) 90° tapered cone angles of the paper. The spray voltage is 4.6 kV.

The spray plume diameter was found to increase with increase in potential. Supplementary Figure S1 shows the spray plume, measured with the Timepix detector, with increasing spray potential for the case of 60° angle tip. It is seen from Fig. S1 that increase in potential leads to increase in diameter of spray plume as well as a de-focusing of the spray plume. The same trend is observed for all paper tip angles. A similar explanation as for electrospray dispersion at higher voltages can be applied to the observed effect.

Visualization of the surface acoustic wave nebulization plume

The charged droplet distribution originating from different designs of SAWN chip has been investigated. An aliquot of 0.5 µL of 1:1 MeOH:H_2O with 10% NH_4OH was deposited on the SAWN chip using a pipette. The arrival of the charged particles is observed over time, until the entire aliquot is consumed. The plume travels over a distance of 1 cm between the SAWN chip and the detector. In the plane of detection the plume has a radial distribution that is spread out over approximately 1 cm^2 with the highest intensity in the center. Data recorded by the Timepix can be presented in different ways to illustrate changes in droplet flux or plume duration and spread.

In Medipix mode all the droplet events are summed in each individual frame, from all frames and present them in a manner similar to a total ion chromatogram. Fig. 4 shows the application of 9 consecutive aliquots. Next to each peak the spray plume footprint of each single aliquot is shown as an inset, the x- and y-axis represent the pixel numbers (256 by 256), and the counts are represented on a colored intensity scale.

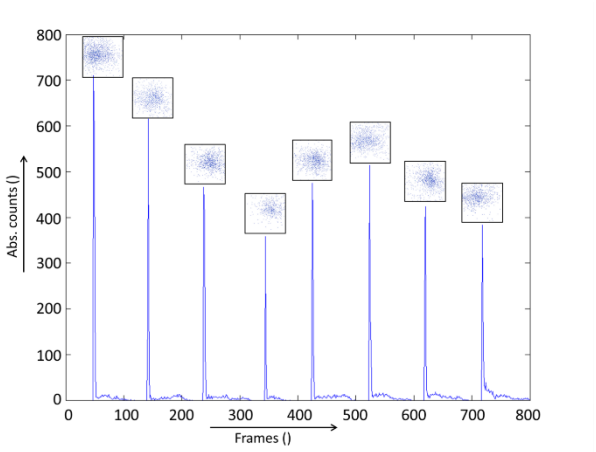

Figure 4 - The total number of counts versus the frame number for a progressive wave chip experiments. The insets show the integrated signal per droplet application.

Alternatively, one can sum all the frames together to present an image illustrating the total cross-section of the plume as it hits the Timepix detector. Using the Timepix to image the charged droplets in the nebulized plume, clear differences can be seen between the plumes generated by the two different SAWN chip designs. Fig. 5 shows the comparison between the droplet plumes generated from the PW chip design and the SW chip design, summed across the complete nebulization of a single 0.5µL aliquot. For both chip designs, viewing the cross-sections of the plumes in this way indicates that the plumes are relatively homogenous from both designs. However, the plume image from the SW chip (see Fig. 5) clearly shows an increase in the number of detected droplets compared to the PW chip which agrees with the TIC style result. It is possible to see that the droplets detected from SW chip plume have spread over a much wider area.

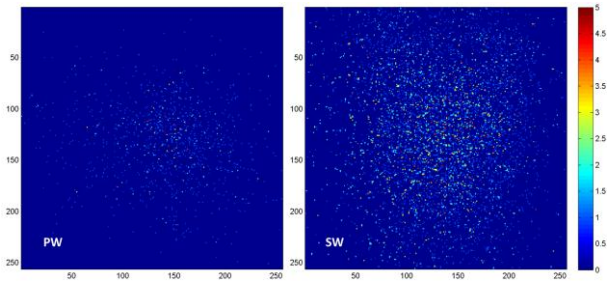

Figure 5 -2D contour maps comparing the spray plume footprint (integrated for 1 aliquot) from a PW chip design with a SW chip design.

The difference in total numbers of events detected by the Timepix between the PW and SW chip designs is one order of magnitude. For the experiments presented in Figures 4 and 5, the electrode “spray” potential was maintained at 800 V.

If the Timepix chip is run in time-over-threshold (ToT) mode, the Timepix measures how long each pixel remains above a pre-set potential threshold. ToT is a measure of how much charge has been detected by each pixel on the Timepix, and thus provides an estimate of the number of elemental charges transferred by the droplets. Using this technique is it possible to determine that there are more charges detected from plumes generated by the SW chip design than from the PW chip design. This result is in agreement with experiments where SAWN is used in combination with mass spectrometry that show an improvement in sensitivity in moving from the PW design to the SW design.

Using this method it is also possible to show that both chip designs produce more charges as the additional “spray” voltage potential is increased. Again, this agrees with the data recorded when using SAWN as a liquid interface for mass spectrometry.

4. CONCLUSIONS

Timepix detectors do not require a vacuum to operate and so are uniquely suited as an ambient detector. In this study we have demonstrated direct charge detection from the droplet plumes emanating from three different ionization methods; ESI, PSI and SAWN.

The Timepix detector gives us a valuable illustration of changes in spatial distribution of the ESI ionization plume with change in spray potential. Lower spray voltages result in an unstable spray and intermediate spray voltages show the best focusing characteristics needed for mass spectrometry. For higher spray voltages the spray becomes dispersed as a consequence of Coulombic repulsion and space charge effects. The results are in agreement with the literature regarding electrospray mass spectrometry.

In case of PSI the most important parameters for improved transmission of ions are the paper tip angle and paper spray potential. We have studied the effect of those parameters on the ionization plume and the results agree with results reported in the literature. The spray has better focusing characteristics at higher tip angles (e.g. 60° and 90°). This is due to intermediate electric fields at the paper tip for higher angles. For higher spray potentials the ion beam splits into multiple beams due to Coulombic repulsion and space charge effects, similar to ESI. Previous results regarding the ion beam diameter for varying paper angle observed with a microscopic camera agree with our observations.

Furthermore we have used the capabilities of the Timepix detector to study two different designs of SAWN liquid interface. The SW SAWN chip design produces more charged droplets than the PW chip design. The Timepix visualizes this and shows the increase in both droplet numbers and in the total numbers of charges. With increased electrode potential an increase in charge transferred by the droplets is detected. The results from the Timepix detector agree with the results seen from the use of SAWN as an ionization source in mass spectrometry that shows the SW design produces a better limit of detection than PW designs.

The benefit of the Timepix detector, in this case is that more information can be gathered on the speed, shape and density of the plumes generated by ambient ionization sources. This information can then be used to develop improved sources and interfaces. Secondly, the Timepix system allows ambient ionization sources to be rapidly tested and developed in facilities which do not or cannot have a mass spectrometer installed for that purpose. This could be useful for quality control or system test purposes for the production of ambient ionization sources.

5. ACKNOWLEDGEMENTS

This work is part of the research programme of the Foundation for Fundamental Research on Matter (FOM), which is part of the Netherlands Organisation for Scientific Research (NWO). We thank J. Visser and M. van Beuzekom for useful discussions. We would like to thank M. Wilson, R. Buijs, D. Spaanderman and R. Struik for technical support and realization of the setups.

6. REFERENCES

[1] J. H. Reynolds. High sensitivity mass spectrometer for noble gas analysis. *Rev. Sci. Instrum.* **1956**, *11*, 928.

[2] G. E. VanLear, F. W. McLafferty. Biochemical aspects of high-resolution mass spectrometry. *Annu. Rev. Biochem.* **1969**, *38*, 289.

[3] R. G. Cooks, Z. Ouyang, Z. Takats, J. M. Wiseman. Ambient Mass Spectrometry. *Science* **2006**, *311*, 1566.

[4] F. P. M. Jjunju, A. Li, A. Badu-Tawiah. In situ analysis of corrosion inhibitors using a portable mass spectrometer with paper spray ionization. *Analyst* **2013**, *138*, 3740.

[5] M. Yamashita, J. B. Fenn. Electrospray ion source. Another variation on the free-jet theme. *J. Phys. Chem.* **1984**, *88*, 4451.

[6] Z. Takáts, J. M. Wiseman, B. Gologan, R. G. Cooks. Mass spectrometry sampling under ambient conditions with desorption electrospray ionization. *Science* **2004**, *306*, 471.

[7] M. Kurosawa, T. Watanabe, A. Futami, T. Higuchi. Surface acoustic wave atomizer. *Sensors Actuators A Phys.* **1995**, *50*, 69.

[8] S. R. Heron, R. Wilson, S. A. Shaffer, D. R. Goodlett, J. M. Cooper. Surface acoustic wave nebulization of peptides as a microfluidic interface for mass spectrometry. *Anal. Chem.* **2010**, *82*, 3985.

[9] Y. Huang, S. H. Yoon, S. R. Heron, C. D. Masselon, J. S. Edgar, F. Tureček, D. R. Goodlett. Surface acoustic wave nebulization produces ions with lower internal energy than electrospray ionization. *J. Am. Soc. Mass Spectrom.* **2012**, *23*, 1062.

[10] S. H. Yoon, Y. Huang, J. S. Edgar, Y. S. Ting, S. R. Heron, Y. Kao, Y. Li, C. D. Masselon, R. K. Ernst, D. R. Goodlett. Surface acoustic wave nebulization facilitating lipid mass spectrometric analysis. *Anal. Chem.* **2012**, *84*, 6530.

[11] D. R. Goodlett, S. R. Heron, J. Cooper. Methods and Systems for Mass Spectrometry. US 2012/0145890 A1, **2012**.

[12] E. E. Dodd. The Statistics of Liquid Spray and Dust Electrification by the Hopper and Laby Method. *J. Appl. Phys.* **1953**, *24*, 73.

[13] M. Von Smoluchowski. Experimentell nachweisbare, der ueblichen Thermodynamik widersprechende Molekularphaenomene. *Phys. Zeitschrift* **1912**, *13*, 1069.

[14] C. R. Blakley, M. L. Vestal. Thermospray interface for liquid chromatography/mass spectrometry. *Anal. Chem.* **1983**, *55*, 750.

[15] M. L. Vestal. Studies of ionization mechanisms involved in thermospray LC-MS. *Int. J. Mass Spectrom. Ion Phys.* **1983**, *46*, 193.

[16] A. Hirabayashi, M. Sakairi, H. Koizumi. Sonic Spray Ionization Method for Atmospheric Pressure Ionization Mass Spectrometry. *Anal. Chem.* **1994**, *66*, 4557.

[17] D. A. Thomas, L. Wang, B. Goh, E. S. Kim, J. L. Beauchamp. Mass Spectrometric Sampling of a Liquid Surface by Nanoliter Droplet Generation from Bursting Bubbles and Focused Acoustic Pulses: Application to Studies of Interfacial Chemistry. *Anal. Chem.* **2015**, *87*, 3336.

[18] J. Liu, H. Wang, N. E. Manicke, J. M. Lin, R. G. Cooks, Z. Ouyang. Development, characterization, and application of paper spray ionization. *Anal. Chem.* **2010**, *82*, 2463.

[19] H. Wang, J. Liu, R. Graham Cooks, Z. Ouyang. Paper spray for direct analysis of complex mixtures using mass spectrometry. *Angew. Chem.* **2010**, *49*, 877.

[20] G. Tepper, R. Kessick. Nanoelectrospray aerosols from microporous polymer wick sources. *Appl. Phys. Lett.* **2009**, *94*, 084106.

[21] R. D. Espy, A. R. Muliadi, Z. Ouyang, R. G. Cooks. Spray mechanism in paper spray ionization. *Int. J. Mass Spectrom.* **2012**, *325-327*, 167.

[22] A. Badu-Tawiah, R. G. Cooks. Enhanced ion signals in desorption electrospray ionization using surfactant spray solutions. *J. Am. Soc. Mass Spectrom.* **2010**, *21*, 1423.

[23] Q. Yang, H. Wang, J. D. Maas, W. J. Chappell, N. E. Manicke, R. G. Cooks, Z. Ouyang. Paper spray ionization devices for direct, biomedical analysis using mass spectrometry. *Int. J. Mass Spectrom.* **2012**, *312*, 201.

[24] S. U. A. H. Syed, G. B. Eijkel, P. Kistemaker. Experimental Investigation of the 2D Ion Beam Profile Generated by an ESI Octopole-QMS System. *J. Am. Soc. Mass Spectrom.* **2014**, *25*, 1780.

[25] A. Kiss, J. H. Jungmann, D. F. Smith, R. M. A. Heeren. Microscope mode secondary ion mass spectrometry imaging with a Timepix detector. *Rev. Sci. Instrum.* **2013**, *84*, 013704.

[26] J. V Iribarne, B. A. Thomson. On the evaporation of small ions from charged droplets. *J. Chem. Phys.* **1976**, *64*, 2287.

[27] M. Dole, L. L. Mack, R. L. Hines, R. C. Mobley, L. D. Ferguson, M. B. Alice. Molecular Beams of Macroions. *J. Chem. Phys.* **1968**, *49*, 2240.

[28] X. Llopart, M. Campbell, D. San Segundo, E. Pernigotti, R. Dinapoli, Medipix2, a 64k pixel read out chip with 55 µm square elements working in single photon counting mode, in *Nuclear Science Symposium Conference Record, 2001*. IEEE, **2001**, pp. 1484–1488.

[29] X. Ã. Llopart, R. Ballabriga, M. Campbell, L. Tlustos, W. Wong. Timepix, a 65k programmable pixel readout chip for arrival time, energy and/or photon counting measurements. *Nucl.*

Instruments Methods Phys. Res. Sect. A Accel. Spectrometers, Detect. Assoc. Equip. **2007**, *581*, 485.

[30] J. H. Jungmann, R. M. A. Heeren. Detection systems for mass spectrometry imaging: A perspective on novel developments with a focus on active pixel detectors. *Rapid Commun. Mass Spectrom.* **2013**, *27*, 1.

[31] J. H. Jungmann, D. F. Smith, A. Kiss, L. MacAleese, R. Buijs, R. M. A. a Heeren. An in-vacuum, pixelated detection system for mass spectrometric analysis and imaging of macromolecules. *Int. J. Mass Spectrom.* **2013**, *341-342*, 34.

[32] J. Vallerga, J. McPhate, A. Tremsin, O. Siegmund, B. Mikulec, A. Clark. Optically sensitive Medipix2 detector for adaptive optics wavefront sensing. *Nucl. Instruments Methods Phys. Res. A* **2005**, *546*, 263.

[33] D. Turecek, T. Holy, J. Jakubek, S. Pospisil, Z. Vykydal. Pixelman: a multi-platform data acquisition and processing software package for Medipix2, Timepix and Medipix3 detectors. *J. Instrum.* **2011**, *6*, C01046.

7. Figures

Figure 1:

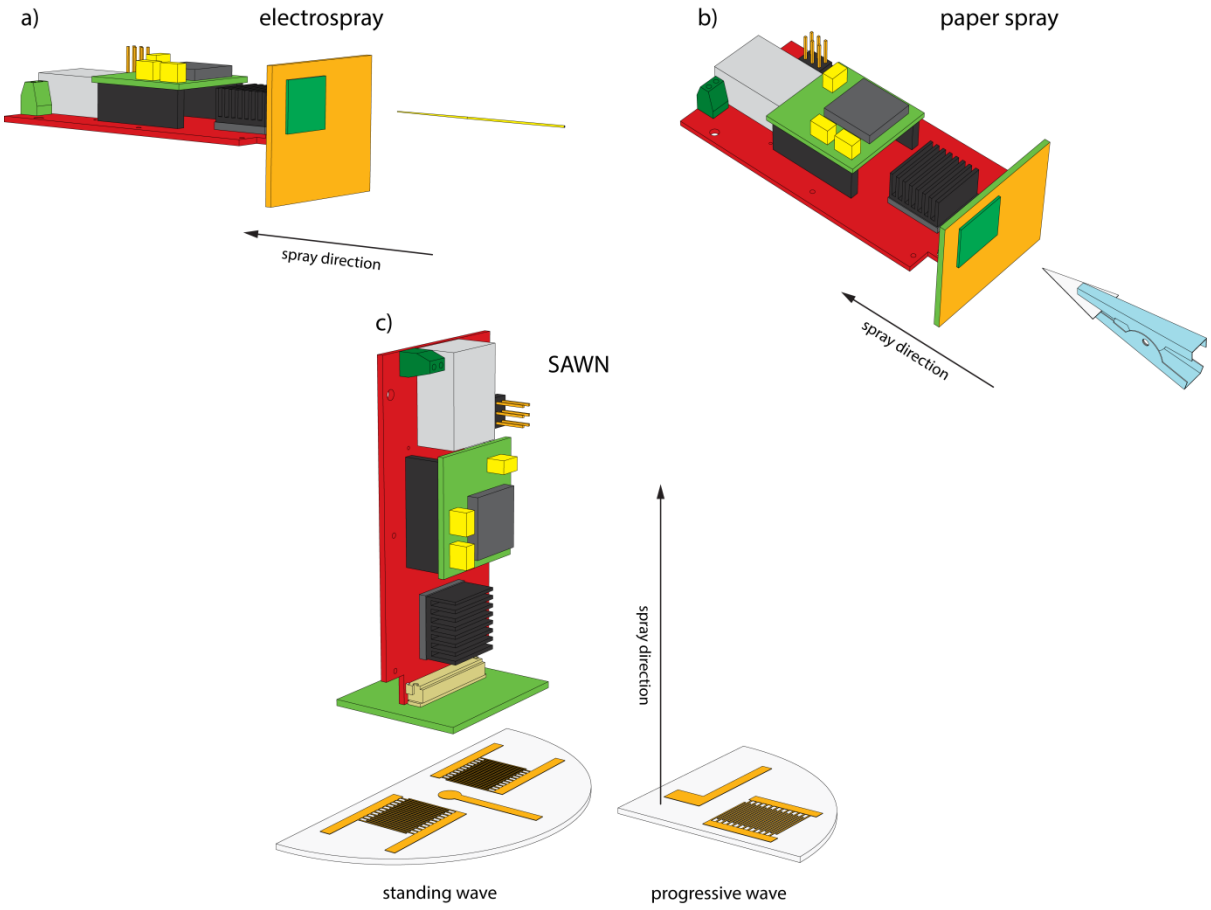

Caption Figure 1:

Illustration of the setups for a) electrospray ionization, b) paper spray ionization, and c) two designs of surface acoustic wave nebulization, progressive wave and standing wave chip design.

Figure 2:

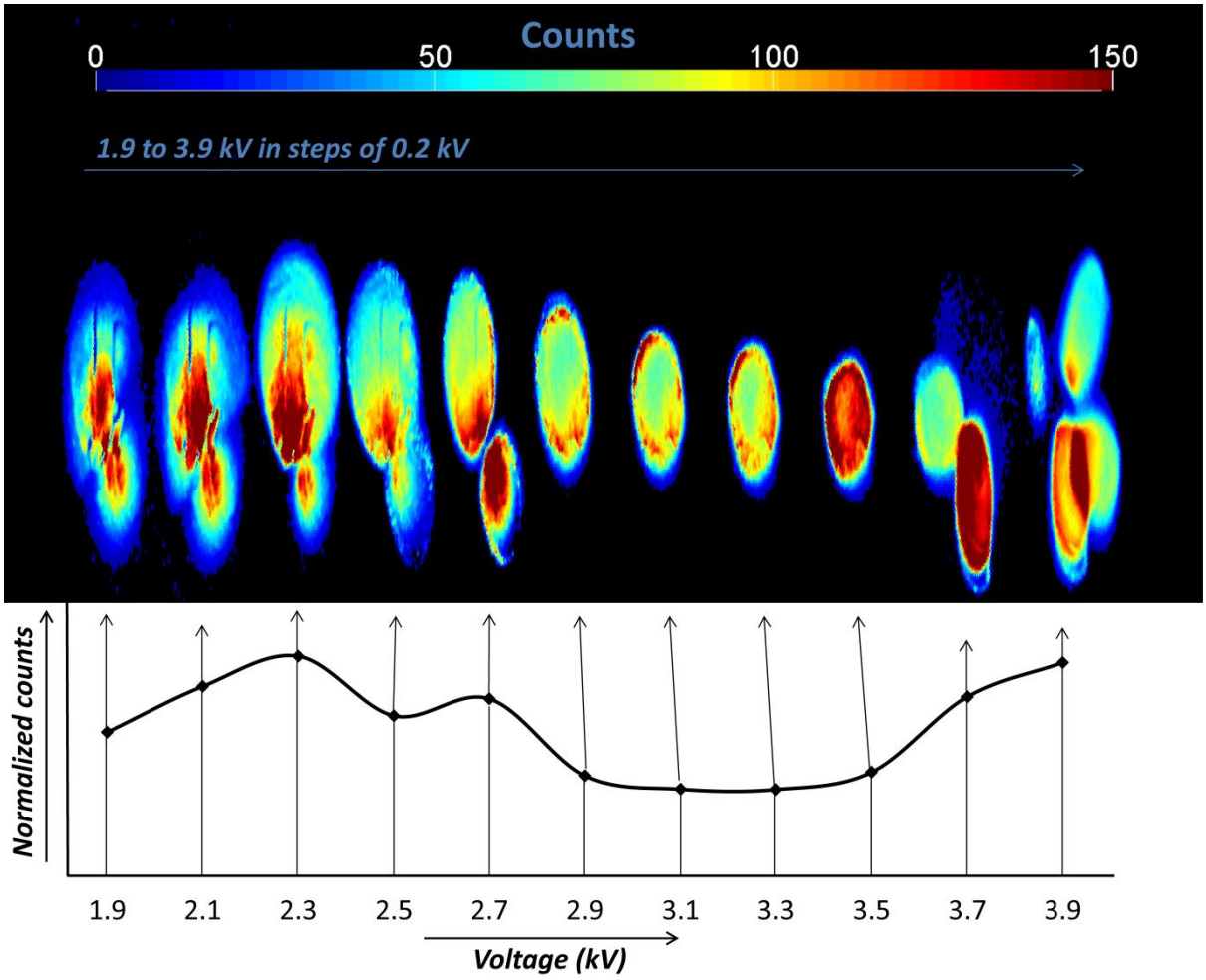

Caption Figure 2:

3D representation of a z-stack of 2D contour maps showing the the development of the ESI ion beam with the spray voltage increasing from 1.9 to 3.9 kV. Counts are represented on a normalized scale with the maximum at 2.3 kV for 294200 counts.

Figure 3:

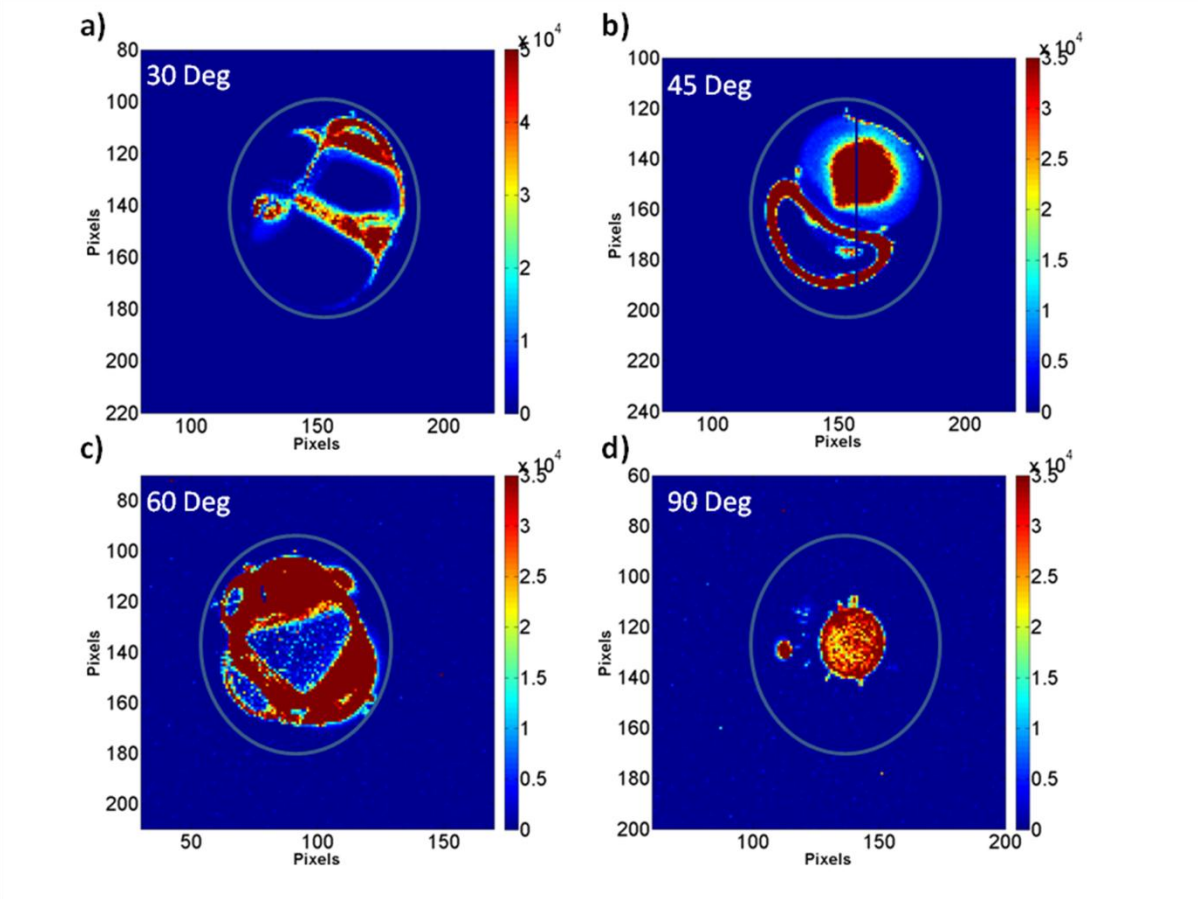

Caption Figure 3: Paper spray ionization plumes observed for a) 30°, b) 45°, c) 60°, and d) 90° tapered cone angles of the paper. The spray voltage is 4.6 kV.

Figure 4:

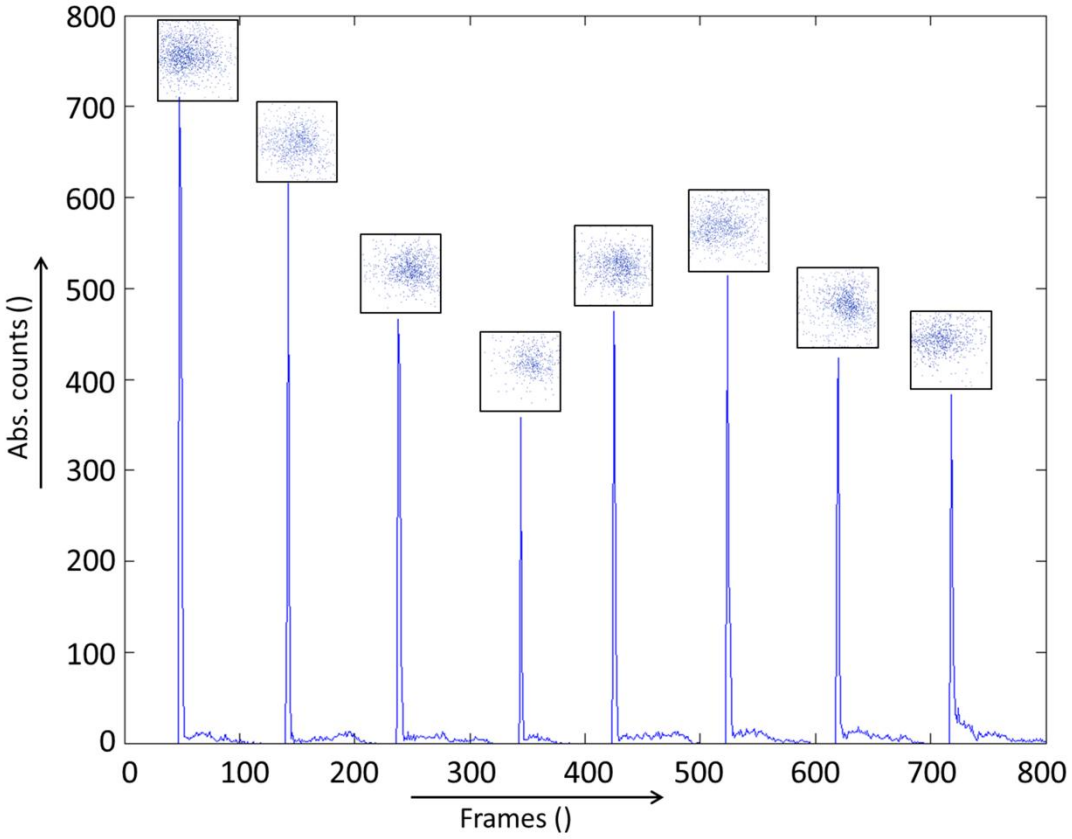

Caption Figure 4: The total number of counts versus the frame number for a progressive wave chip experiments. The insets show the integrated signal per droplet application.

Figure 5:

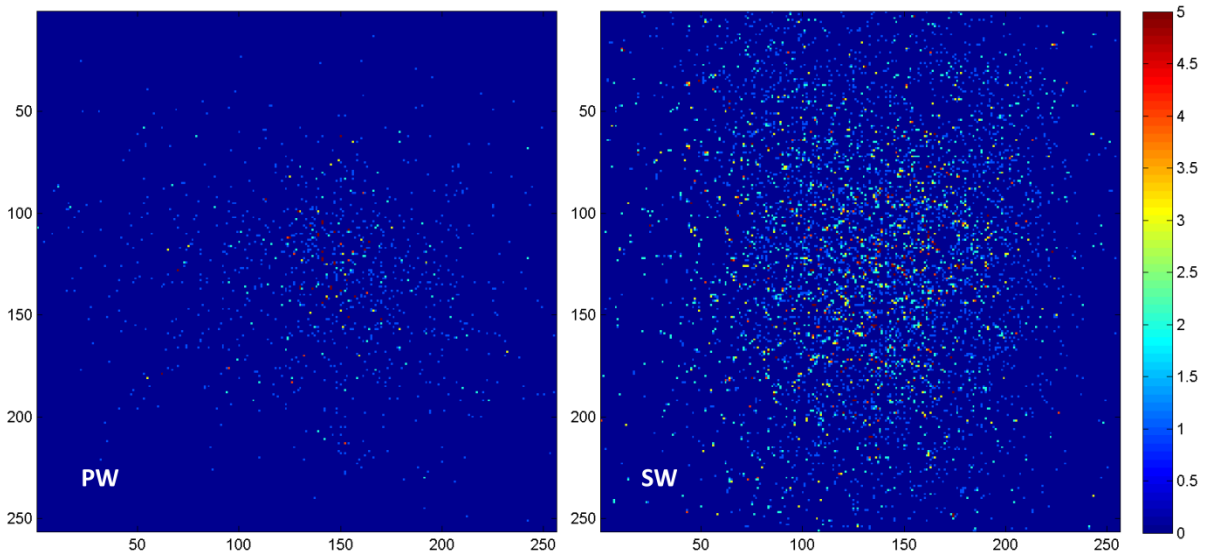

Caption Figure 5: 2D contour maps comparing the spray plume footprint (integrated for 1 aliquot) from a PW chip design with a SW chip design.

Supporting Info

Figure S1:

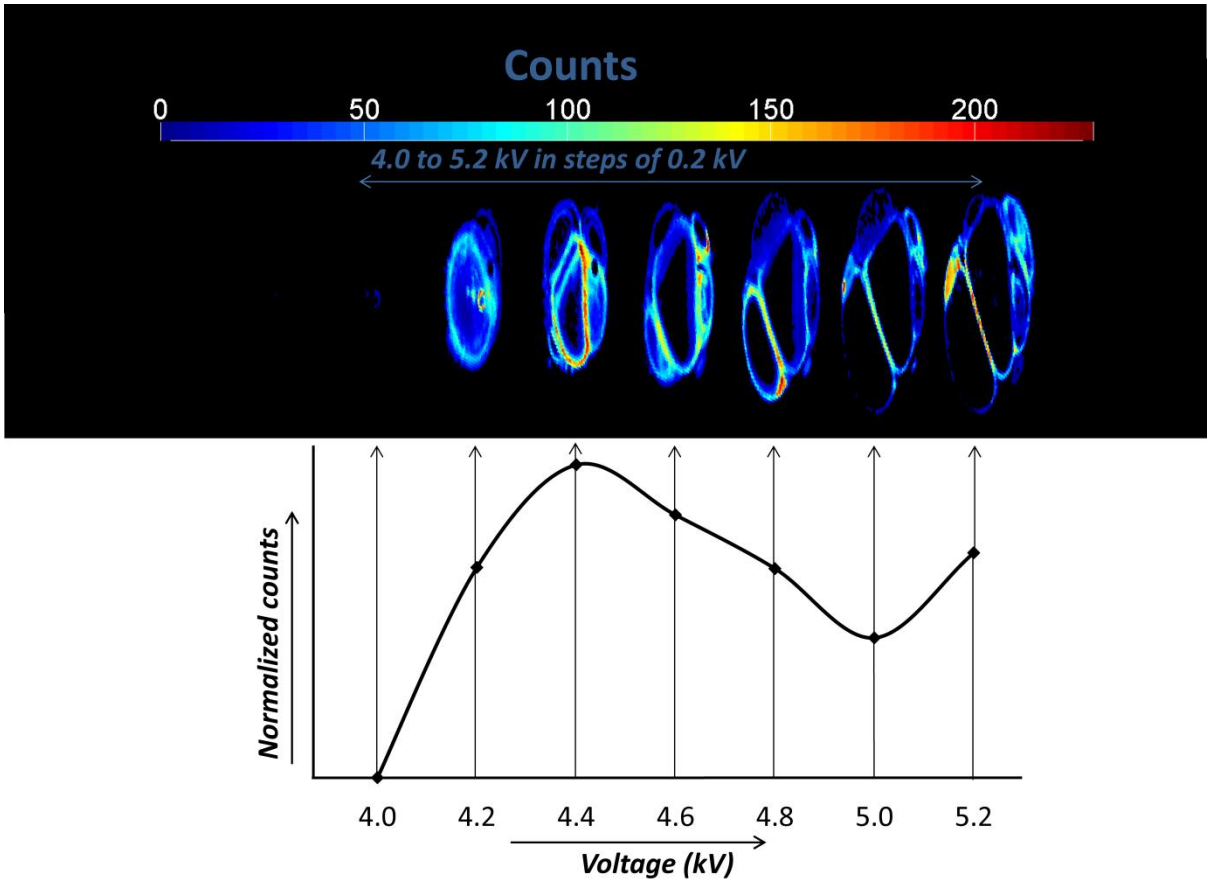

Caption Figure S1:

3D representation of a z-stack of 2D contour maps showing the the development of the PSI ion beam with the spray voltage increasing from 4.0 to 5.2 kV. Counts are represented on a normalized scale with the maximum at 4.4. kV for 136469 counts. The angle of the paper is 60°.